Asian Journal of Chemistry; Vol. 33, No. 11 (2021), 2621-2625

ASIAN JOURNAL OF CHEMISTRY

https://doi.org/10.14233/ajchem.2021.23346

Microwave Assisted Chemical Modification of Graphite Oxide for Supercapacitor Application

R. SIDDHARTHAN[1], P. MAHALINGAM[1,*], E. KANAGARAJ[1] and K. SARAVANAN[2]

[1]Department of Chemistry, Arignar Anna Government Arts College, Namakkal-637002, India
[2]Department of Chemistry, Thiruvalluvar Government Arts College, Rasipuram-637401, India

*Corresponding author: E-mail: ponmahanano@gmail.com

Received: 29 May 2021; *Accepted*:16 July 2021; *Published online*: 20 October 2021; AJC-20539

In present work, graphite oxide was chemically modified with boron, nitrogen and sulfur co-doping in a simple, single step green method by microwave treatment. Borax, urea and thiourea were used as precursors for doping. Mixtures of graphite oxide with precursors were microwave treated using domestic microwave oven at 800 W for 5 min. The products obtained were characterized for its morphology, structure, composition and electrical properties. The results showed that simultaneous reduction of graphite oxide and doping of boron, nitrogen and sulfur were occurred. The elemental doping distorts the structure without much affecting the crystalline nature. The boron, nitrogen and sulfur elements were doped in graphite oxide to the extent of 9.97 at%, 2.67 at% and 0.84 at%, respectively. The cyclic voltammetry and electrochemical impedance spectroscopy studies showed that boron, nitrogen and sulfur co-doped graphite oxide could be a suitable material for supercapacitor application.

Keywords: Graphite oxide, Chemical modification, Doping, Microwave, Supercapacitor.

INTRODUCTION

Graphite, one of carbon allotropes, which exists as stacked layers, is exfoliated in to graphite oxide. The functionalized graphite oxide shows enhanced properties. Graphite oxide is functionalized by many methods such as microwave, sol-gel and ball milling [1-3]. The oxygen functionalization hinders the electrical and thermal properties in graphite. These drawbacks are overcome by reducing graphite oxide without restacking. The reduced graphite oxide is found to be a potential material for many applications primarily due to its high surface area [4].

Studies indicated that elements such as boron, nitrogen, sulfur, fluorine, phosphorous could be incorporated into graphene layer. These doping elements modify surface area, electrical, thermal and mechanical properties of graphene material. Synthesis, structure and properties of boron and nitrogen doped graphene have also been reported earlier [4-6]. Microwave heating is proposed as a quick and efficient approach to prepare nitrogen doped graphene in NH_3 atmosphere. The result showed that graphene as a good microwave absorbing material, can raise high temperature in minutes, which makes possible for nitrogen incorporation into lattice structure under NH_3 environment. Elemental analysis and X-ray photoelectron spectroscope (XPS) are used to verify nitrogen doping and found with nitrogen content of 5.04 wt% [7]. Band gap and electron transport properties of graphene are tuned by boron doping through reaction with trimethyl boron decomposed by microwave plasma. The report showed that boron atoms are substitutionally incorporated into graphenes without segregated boron domains. The boron content in the material was in a range of 0-13.85 atom % [8].

Reduction and doping of graphene oxide are simultaneously achieved through a downstream microwave plasma source and the process negates need for high temperatures and toxic solvents that normally associated with existing methods. This gas phase low temperature process is completely dry and thus minimizes aggregation of graphene layers which normally occurs in liquid phase reduction methods [9]. Preparation of nitrogen doped graphene nanosheets using sodium amide as a nitrogen source by simple microwave irradiation has been reported. Exfoliation and nitrogen doping of graphite simultaneously occurred during microwave irradiation. Doped nitrogen content in the material reached to 8.1% [10]. The sulfur doped

graphite was prepared from concentrated sulfuric acid-graphite intercalation compounds by solid state microwave irradiation [11]. Microwave-assisted heating method was used to dope graphite oxide, pyrolytic graphene oxide and hydrogen-reduced pyrolytic graphene oxide [12]. Nitrogen doped graphite oxide with or without holes are controllably, directly and rapidly fabricated from graphite powder *via* one step one pot microwave assisted reaction [13]. Nasini *et al*. [14] prepared phosphorous and nitrogen dual heteroatom doped mesoporous carbon *via* microwave method for supercapacitor application. Varying the amount of tannin to melamine in the carbonization process produced varying nitrogen, phosphorus and oxygen content. Nitrogen is introduced into carbon particles *via* addition of urea solution during microwave-assisted hydrothermal carbonization. The nitrogen content is controlled by varying the urea concentration [15].

Boron, nitrogen and sulfur tri-doped carbon quantum dots are prepared by hydrothermal method using boric acid and L-cysteine as precursors and further immobilized on graphite oxide in presence of a cobalt precursor to synthesize a nanocomposite of cobalt oxide and B, N, S tri-doped graphite oxide [16]. Crystalline boron and nitrogen co-doped microwave assisted reduced graphene oxide film is investigated as a potential transparent conducting electrode material. X-ray diffraction results revealed good crystalline of film and presence of few small domains of hexagonal boron nitride in microwave assisted reduced graphene oxide sheets under the co-doping process [17]. Also, microwave-assisted strategy is developed to synthesis nitrogen and boron co-doped graphene with a hierarchical framework [18]. Though several methods are adopted to synthesize doped graphite layers, these methods involve tedious process setup and post treatment requirements. In this work, the graphite oxides co-doped with combinations of boron, nitrogen and sulfur were synthesized by using microwave treatment without use of toxic reducing agents.

EXPERIMENTAL

The analytical grade reagents were used in these experiments. The graphite oxide precursor was prepared from graphite flakes by modified Hummers method [19]. Graphite flakes as precursor material (2.0 g) was mixed with 150 mL of conc. sulphuric acid under constant stirring. The mixture was cooled to 0 ºC using an ice bath with a constant stirring. To a cold mixture, $KMnO_4$ (10.0 g) was carefully added with constant stirring, maintaining the temperature of the mixture below 20 ºC for 1 h. The mixture was then added with 100 mL distilled water then maintained at 85 ºC for 1 h. To a mixture, 200 mL water and 40 mL 30% H_2O_2 were added slowly and stirred for 30 min at 35 ºC. The mixture was centrifuged at 2000 rpm for 20 min and washed with distilled water repeatedly till all the unwanted ions were removed. Finally, the obtained graphite oxide was dried in air oven at 110 ºC for 24 h.

The co-doping of boron, nitrogen and sulfur elements on graphite oxide layer and its properties were investigated. The precursors were selected based on green chemistry principles for co-doping. The boric acid is chosen as a precursor for boron doping while thiourea was selected for doping nitrogen and sulfur. Graphite oxide (1.0 g) was dispersed in ethanol (20 mL) under constant stirring and ultrasonication process. A boric acid (2 mg/mL) and thiourea (2 mg/mL) were mixed with the GO dispersion under stirring conditions and sonicated for 3 h. The boron, nitrogen and sulfur co-doped graphite oxide was synthesized using microwave assisted heating method by irradiating the microwave produced with 800 W for 5 min with stirring and grinding for every 30 s. The mixture was then washed using deionized hot water to remove the impurities and then dried at 80 ºC. The structural, morphological and electrical properties of the material were characterized using SEM, TEM, XRD, Raman, XPS and cyclic voltammetry techniques.

RESULTS AND DISCUSSION

Morphology studies: The morphology of prepared graphite oxides doped with boron, co-doped with boron and nitrogen (BN) and co-doped with boron, nitrogen and sulfur (BNS) elements were studied using SEM technique. It can be seen from the (Fig. 1) that boron, BN and BNS doped graphite layers were all thin and having no crack or hole. The graphite oxide layers were exfoliated during the doping process under microwave treatment. It was visually observed during the doping process that doping using borax and thiourea showed good exfoliation compared to the borax alone or borax with urea. Moreover, SEM image (Fig. 1c) also reflected that graphite oxide sheets were thin and wrinkle indicating the reduced aggregation of exfoliated graphite oxide layers.

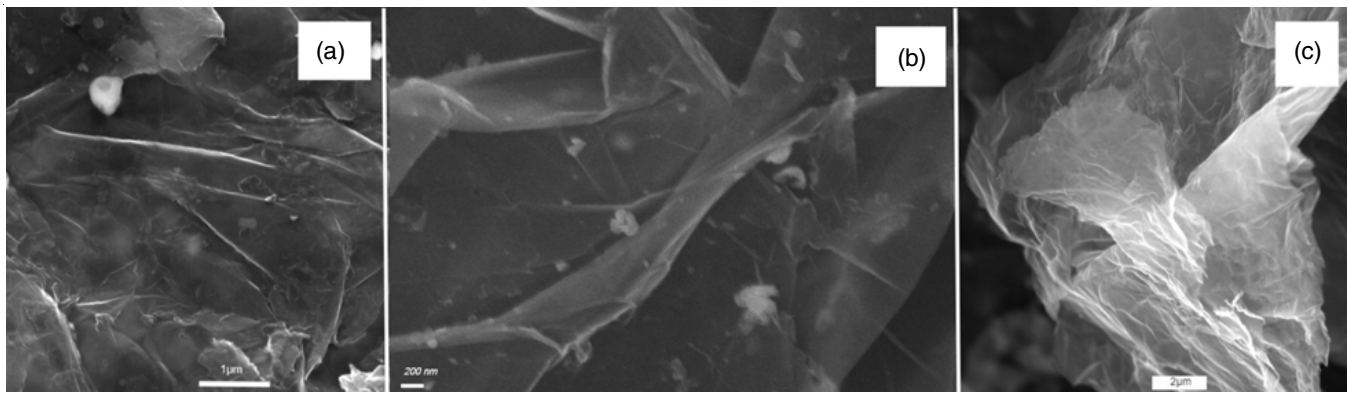

Fig. 1. SEM image (a) B doped rGO, (b) BN doped rGO, (c) BNS doped rGO

The TEM images recorded for the material prepared using borax and thiourea (Fig. 2a) indicates that the graphite layers were well exfoliated and aggregation of layers was reduced even after microwave treatment. The transparent nature of TEM image reveals that the material contains few layers only. Moreover, the layers are with fewer wrinkles and fold. The selected area electron diffraction (SAED) pattern recorded for BNS doped reduced graphite oxide is shown in Fig. 2b, which provides additional information that inter-planar distance d_{002} for the material is 0.36 nm. The graphene sheet exhibited slightly broader but clear diffraction pattern. This indicates B, N and S co-doped graphite oxide differ from the pristine graphite layers. The SAED analysis of B, N and S co-doped graphite layer shows atomic % of elements carbon 85.26%, oxygen 1.25%, boron 9.97%, nitrogen 2.67% and sulfur 0.84%. It was found that oxygen content in doped graphite is much lower than that of undoped graphite oxide. This indicates that graphite oxide is reduced during doping under microwave treatment. The hydroxyl, epoxy and carbonyl groups are reduced simultaneously while boron, nitrogen and sulfur were doped. The elemental percentage obtained from SAED patterns (not shown) recorded for the material B doped rGO was carbon 83.59%, oxygen 3.2%, boron 13.21% and for BN doped rGO was carbon 86.58%, oxygen 2.31%, boron 6.38%, nitrogen 4.72%, respectively.

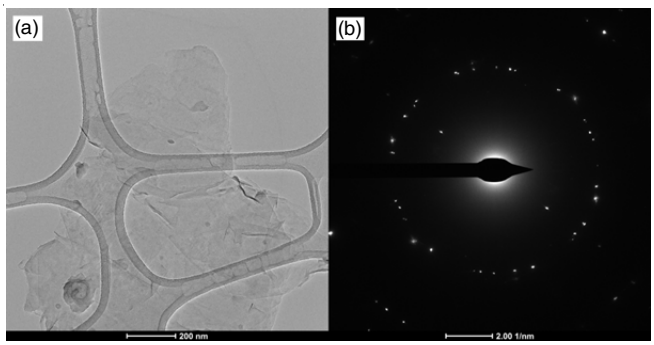

Fig. 2. BNS doped rGO (a) TEM image (b) SAED pattern

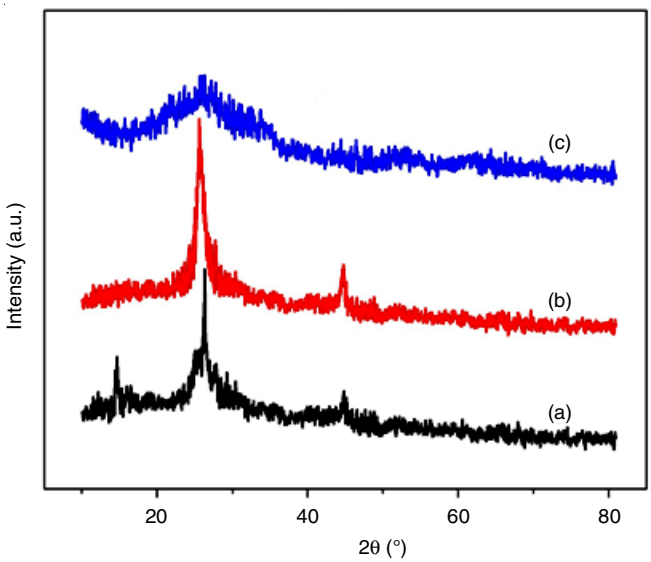

Fig. 3. XRD pattern of (a) B doped rGO, (b) BN doped rGO, (c) BNS doped rGO

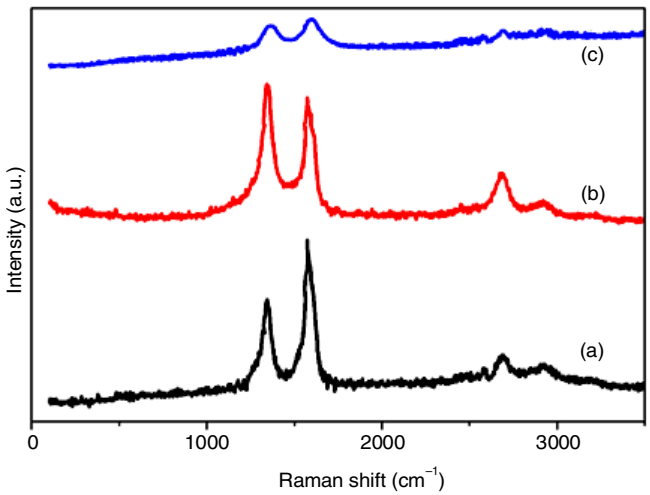

Fig. 4. Raman scattering pattern of (a) B doped rGO, (b) BN doped rGO, (c) BNS doped rGO

XRD studies: The XRD pattern (Fig. 3a) shows two broad and low intensive diffraction peaks over the range 2θ = 20-26º and 43-44º, which are attributed to (002) and (100) planes, respectively. The higher relative intensity of lower angle peak corresponds to (002) plane than that of the plane (100) indicates the disorder in the graphite layer. Inter planar distance calculated for 2θ peak at 26.28 is 0.339 nm. An increase of FWHM value for the BNS co-doped graphite oxide supports the well exfoliation during experiments and less restacking with more disordered or strained structure. The more disorder and strain produced in graphite oxide structure is attributed to doped sulfur element.

Raman studies: The Raman spectrum recorded for boron, BN and BNS co-doped reduced graphite oxide are shown in Fig. 4. The spectrums show the characteristic peaks D and G corresponding to defects and crystalline nature, respectively. The I_G/I_D ratio calculated for the materials boron, BN and BNS co-doped reduced graphite oxide were 1.47, 0.87 and 0.77, respectively. Slightly higher intensity of D peak than G peak for BNS co-doped material indicates that the material retains the crystalline with some disorder, which may be due to the doped B, N and S elements. These elements on doping at carbon structure distort the orderly arrangement of carbon atoms in the graphite structure and thus introduce disorder in the structure.

XPS studies: The composition of boron, nitrogen and sulfur in the graphite layer was analyzed using X-ray photoelectron spectroscopy (XPS). The XPS spectrum (figure not shown) indicates the presence of C, B, N, S and oxygen elements in material. The peak at 396.4 eV was assigned to B1s signal. The B1s XPS spectrum is deconvoluted into three peaks. The peaks located at 398.2, 399.3 and 401.6 eV can be assigned to boron-nitrogen, boron-carbon and boron-oxygen bond, respectively. Thus boron was incorporated successfully into the graphite layers. The C1s spectrum was deconvoluted into four peaks at 284.3, 285.2, 286.9 and 288.6 eV. The more intense peak at 284.3 eV was assigned to C-C bond while peaks at 285.2 eV

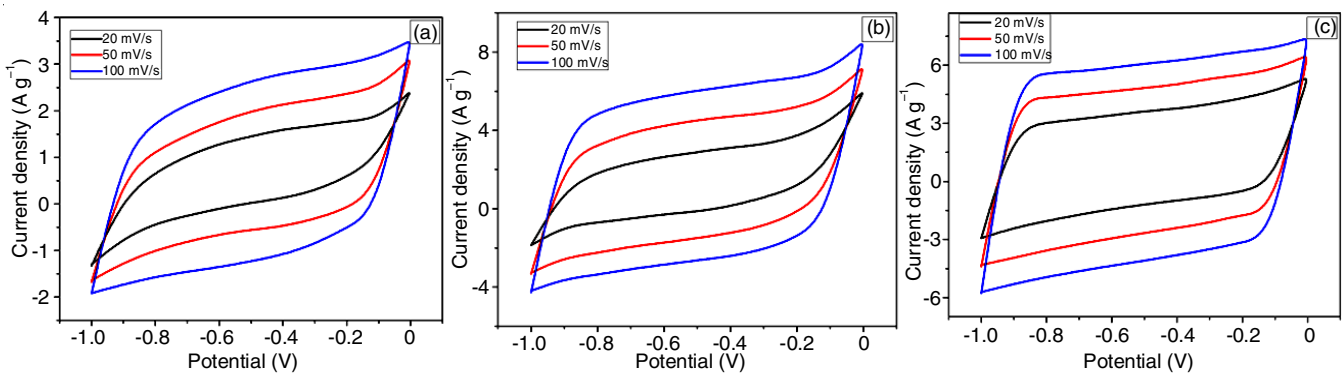

Fig. 5. Cyclic voltammogram (a) B doped rGO, (b) BN doped rGO, (c) BNS doped rGO

and 286.9 eV, which assigned to C-N and C-S bond, respectively. The elemental compositions in the prepared materials were calculated from the XPS spectra. Boron doped rGO contain 11.23% boron, BN doped rGO contains 6.12% boron and 4.35% nitrogen and BNS doped rGO contains 8.9% boron, 2.32% nitrogen and 0.84% sulfur. The elemental compositions were comparable with the results obtained from elemental analysis using SAED.

Cyclic voltammetry: The cyclic voltamograms for the materials boron, BN and BNS co-doped rGO were recorded in a potential window from -1.0 to 0 V *versus* SCE in 6 M KOH electrolyte. Fig. 5 shows the CV curves of materials at different scanning rates 20, 50 and 100 mV s^{-1}. The CV curve shows nearly symmetrical shape with no redox peaks. Increase in scan rate results in the slight distortion. This can be attributed to internal resistance of current collector/electrolyte interface [20]. Specific capacitance calculated for the materials were 46, 97 and 124 F g^{-1}. Compared with the boron doped rGO and BN doped rGO, BNS doped rGO shows higher specific capacitance due to the easily accessible surface formed through exfoliation of graphite oxide without restacking. The absence of redox peaks signifies that specific capacitances of the materials are wholly contributed through electrical double layer formation.

EIS studies: The electrochemical impedance spectroscopy (EIS) is used to study the characteristics of electron transfer and recombination process at electrode/electrolyte interface. The Nyquist plot, generally, shows as smaller semi-circle in high-medium frequency region and a Warburg type vertical line in low frequency region [21]. Electrochemical impedance spectroscopy analysis of boron, BN and BNS co-doped graphite oxide materials are shown as Nyquist plot in Fig. 6. The plot shows semi-circles in high-medium frequency region. The impedance curve of boron, BN and BNS co-doped graphite oxide materials intercept the real value represented as *x*-axis. The intercept of the curve with *x*-axis correlated with equivalent series resistance ESR, which indicates the resistance of bulk electrolyte solution. The magnitude of ESR limits the energy efficiency of the electrochemical cell. The lower ESR values for these materials indicate good electrical conductivity of material which is attributed to doped elements and reduced nature of graphite oxide. The conductance and charge transfer tendency of the materials are indicated by the radius of semi-circle. The semi-circle diameter for the materials shows that

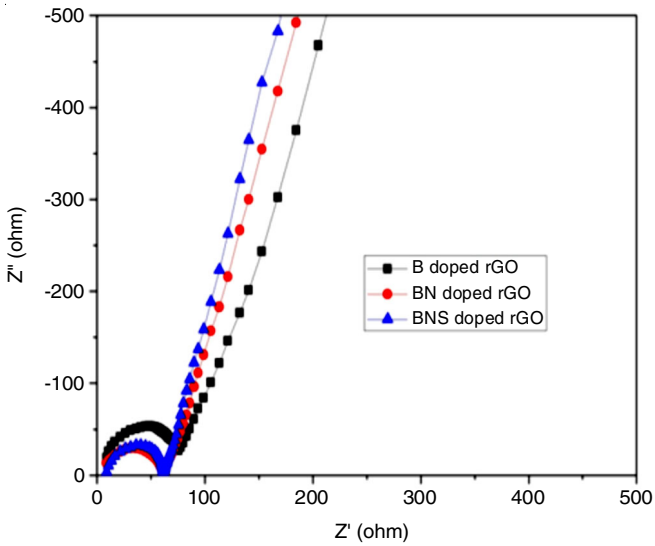

Fig. 6. Electrochemical impedance spectrum of B, BN and BNS doped rGO

BN and BNS doped rGO is lower than boron doped rGO. The smaller semi-circle formation can be attributed to presence of defects due to doping. Moreover, the Warburg line of boron, BN and BNS co-doped graphite oxide material appeared in low frequency region with more than 45° angle indicates that the electrodes performance are controlled by ion diffusion. The cyclic stability of materials was measured at 3 mA over 200 cycles. The observed capacitance for 200 cycles indicated that BNS doped graphite oxide exhibits 85% retention compared with boron doped (76%) and BN doped (80%) graphite oxides. The results indicate that BNS co-doped graphite oxide material exhibits high energy efficiency which is attributed to synergistic effect of the doped elements and effective reduction of graphite oxide during microwave treatment.

Also, it is well known that, when elements are doped in graphene lattice, some carbon atoms are replaced by these elements, which results in defective lattice. The perfect arrangement of carbon atoms in pure graphene gets disturbed on doping and thus the layers are structurally distorted [22]. Moreover, introduction of elements with different electronegative nature such as B, N and S atoms induces more defects due to difference in number of valence electrons of the atoms [23]. As a result, the hybridization of carbon atoms adjacent to these defect sites is disturbed and thus influences the electrical properties.

Conclusion

A microwave treatment method, a simple and single step approach, accede to green chemistry principles, is found to be suitable for the preparation of boron, nitrogen and sulfur co-doped graphite oxide. Graphene oxide reduction and doping were found to occur simultaneously under the experimental conditions. The graphite oxide layers exfoliated during doping process under microwave treatment were with wrinkle and folds indicating the reduced aggregation of exfoliated graphite oxide layers. Doping on carbon structure distorts the graphite structure with retention of crystallinity. The composition of boron, nitrogen and sulfur elements in the material prepared by microwave treatment was found to be about 9.97%, 2.67% and 0.84%, respectively. Specific capacitance of the material arises due to electrical double layer capacitance. The results indicate that synergistic effect of dope elements boron, nitrogen and sulfur with graphite oxide results in high capacitance, energy efficiency and cycle stability.

ACKNOWLEDGEMENTS

The authors acknowledge UGC (MRP-5394/14 (SERO/UGC) March 2014) for instrumental facility. The authors also thank Alagappa University, Karaikudi and Gandhigram University, Dindigul, Centre for Nano and Soft Matter Sciences (CeNS), Bangalure, India for the material characterization analysis.

CONFLICT OF INTEREST

The authors declare that there is no conflict of interests regarding the publication of this article.

REFERENCES

1. A.T. Dideikin and A.Y. Vul, *Front. Phys*., **6**, 149 (2019); https://doi.org/10.3389/fphy.2018.00149
2. Y. Wang, S. Li, H. Yang and J. Luo, *RSC Adv*., **10**, 15328 (2020); https://doi.org/10.1039/D0RA01068E
3. P.P. Briseboisa and M. Siaj, *J. Mater. Chem. C*, **8**, 1517 (2020); https://doi.org/10.1039/C9TC03251G
4. L.S. Panchakarla, K.S. Subrahmanyam, S.K. Saha, A. Govindaraj, H.R. Krishnamurthy, U.V. Waghmare and C.N.R. Rao, *Adv. Mater.*, **21**, 4726 (2009); https://doi.org/10.1002/adma.200901285
5. S. Elumalai, C.-Y. Su and M. Yoshimura, *Front. Mater*., **6**, 216 (2019); https://doi.org/10.3389/fmats.2019.00216
6. F.H. Baldovino, A.T. Quitain, N.P. Dugos, S.A. Roces, M. Koinuma, M. Yuasa and T. Kida, *RSC Adv.*, **6**, 113924 (2016); https://doi.org/10.1039/C6RA22885B
7. Y. Xin, J. Liu, X. Jie, W. Liu, F. Liu, Y. Yin, J. Gu and Z. Zou, *Electrochim. Acta*, **60**, 354 (2012); https://doi.org/10.1016/j.electacta.2011.11.062
8. Y.B. Tang, L.C. Yin, Y. Yang, X.H. Bo, Y.L. Cao, H.E. Wang, W.J. Zhang, I. Bello, S.T. Lee, H.M. Cheng and C.S. Lee, *ACS Nano*, **6**, 1970 (2012); https://doi.org/10.1021/nn3005262
9. N.A. Kumar, H. Nolan, N. McEvoy, E. Rezvani, R.L. Doyle, M.E.G. Lyons and G.S. Duesberg, *J. Mater. Chem. A Mater. Energy Sustain.*, **1**, 4431 (2013); https://doi.org/10.1039/c3ta10337d
10. K.H. Lee, J. Oh, J.G. Son, H. Kim and S.S. Lee, *ACS Appl. Mater. Interfaces*, **6**, 6361 (2014); https://doi.org/10.1021/am405735c
11. F. Li, W. Xu, L. Lu, K. Zhou and Z. Xia, *Chem. Phys. Lett.*, **731**, 136615 (2019); https://doi.org/10.1016/j.cplett.2019.136615
12. P. Tang, G. Hu, Y. Gao, W. Li, S. Yao, Z. Liu and D. Ma, *Sci. Rep.*, **4**, 5901 (2015); https://doi.org/10.1038/srep05901
13. M. Patel, W. Feng, K. Savaram, M. R. Khoshi, R. Huang, J. Sun, E. Rabie, C. Flach, R. Mendelsohn, E. Garfunkel and H. He, *Small*, **11**, 3358 (2015); https://doi.org/10.1002/smll.201403402
14. U.B. Nasini, V.G. Bairi, S.K. Ramasahayam, S.E. Bourdo, T. Viswanathan and A.U. Shaikh, *J. Power Sources*, **250**, 257 (2014); https://doi.org/10.1016/j.jpowsour.2013.11.014
15. A. Jung, S. Han, T. Kim, W.J. Cho and K.H. Lee, *Carbon*, **60**, 307 (2013); https://doi.org/10.1016/j.carbon.2013.04.042
16. S.B. Ingavale, I.M. Patil, H.B. Parse, N. Ramgir, B. Kakade and A. Swami, *New J. Chem.*, **42**, 12908 (2018); https://doi.org/10.1039/C8NJ01138A
17. S. Umrao, H. Mishra, A. Srivastava and S. Lee, *Appl. Phys. Lett.*, **111**, 023106 (2017); https://doi.org/10.1063/1.4993156
18. G.H. Yang, Y.H. Zhou, J.J. Wu, J.T. Cao, L.L. Li, H.Y. Liu and J.J. Zhu, *RSC Adv.*, **3**, 22597 (2013); https://doi.org/10.1039/c3ra44284e
19. W.S. Hummers Jr. and R.E. Offeman, *J. Am. Chem. Soc.*, **80**, 1339 (1958); https://doi.org/10.1021/ja01539a017
20. D. Puthusseri, V. Aravindan, S. Madhavi and S. Ogale, *Energy Environ. Sci.*, **7**, 728 (2014); https://doi.org/10.1039/C3EE42551G
21. N. Parveen, M.O. Ansari, S.A. Ansari and M.H. Cho, *J. Mater. Chem. A*, **4**, 233 (2016); https://doi.org/10.1039/C5TA07963B
22. Y. Zhang, J. Ge, L. Wang, D. Wang, F. Ding, X. Tao and W. Chen, *Sci. Rep.*, **3**, 2771 (2013); https://doi.org/10.1038/srep02771
23. C. Van Pham, M. Klingele, B. Britton, K.R. Vuyyuru, T. Unmuessig, S. Holdcroft, A. Fischer and S. Thiele, *Adv. Sustain. Syst.*, **1**, 1600038 (2017); https://doi.org/10.1002/adsu.201600038